ELSEVIER

Chemical Engineering Journal 79 (2000) 113–122

Chemical Engineering Journal

www.elsevier.com/locate/cej

Cancellation of heat effects in catalytic distillation

Veikko J. Pohjola*, Juha Tanskanen

Department of Process Engineering, University of Oulu, PO Box 4300, FIN-90401 Oulu, Finland

Received 22 September 1998; received in revised form 10 March 2000; accepted 21 March 2000

Abstract

Heat effects in distillation, especially those caused by unequal heats of vaporization of components and highly nonadiabatic operation, were shown in earlier papers to cancel favorably in binary distillation when measuring and computing composition profiles along column height. We show here that the same favorable cancellation takes place in multicomponent catalytic distillation where heat effects are caused by a release or consumption of heat of reaction. A generic profile in terms of pseudo-composition of vapor, solved analytically by applying the linearized theory of multicomponent mass transfer, is given for exothermic reactions as a function of two dimensionless parameters, an eigenvalue of the number of mass transfer units matrix and an eigenvalue of the mass transfer rate factor matrix. Comparison with the solution that ignores the heat effects completely is made in terms of both pseudo-composition and actual composition. The final conclusion of the study is that nonequimolarity can be safely ignored in most practical cases of multicomponent catalytic distillation when computing bulk compositions on a plate in the reaction zone of a column.

Keywords: Reactive distillation; Catalytic distillation; Heat effects; Multicomponent mass transfer; Linearized theory; Composition profile

1. Introduction

Reactive distillation is an exemplar of process where the aim is to simultaneously make more than one phenomenon advance as desired within a single piece of equipment instead of separately in interconnected subprocesses. In addition to a simplified process topology, there are other benefits to be gained from such multiphenomenon processes through coupling effects, as exemplified by certain applications in reactive distillation. For instance, a liquid phase reaction can be kept at a favorable distance from equilibrium by carrying out the reaction at the boiling temperature and by letting a volatile product component vaporize as it is formed. Also, an azeotrope may be broken by introducing into a column a component which reacts with one of the components constituting the azeotrope. Whatever the benefits are, successful control of coupled phenomena requires detailed knowledge of their individual mechanisms and consequent understanding of how their rates and extents interfere. Solving mathematical models for simulating multiphenomenon processes is tedious due to the complex interdependencies within the models. Accordingly, considerable efforts are currently devoted to developing algorithms capable of solving effectively rate-based models of reactive distillation. Any simplification which reduces the degree of interdependence inherent in such models without simultaneous loss of realism would be a meaningful step forward in the design methodology of multiphenomenon processes.

When a chemical reaction takes place in a distillation column, there is always an associated release or consumption of heat. In certain applications of current industrial value the reactions take place at the surface of a solid catalyst, which is in contact with the boiling liquid, and are highly exothermic. In such cases, the heat released causes excess vaporization at the vapor–liquid interface. Mass transfer across the interface becomes highly nonequimolar, which has a dramatic effect on the molar fluxes of components across the interface. The molar flows of liquid and vapor are naturally affected accordingly.

While ‘heat effects’ is a much discussed topic in the distillation literature, the context in the past has most often been the validity of the assumption of equimolar countertransfer and the utility of the McCabe–Thiele diagram. Heat effects have usually referred to unequal molar heats of vaporization of components, heat of mixing, and heat losses. In the case of a highly exothermic (endothermic) reaction taking place in one phase, the deviation from equimolarity due to excessive heat introduced (removed) can be orders of magnitude higher than in conventional distillation. Hence the familiar reasoning for ignoring the heat effects does not apply.

* Corresponding author. Tel.: +358-8-553-2357; fax: +358-8-553-2304.
E-mail address: veikko.pohjola@oulu.fi (V.J. Pohjola)

1385-8947/00/$ – see front matter
PII: S1385-8947(00)00163-7

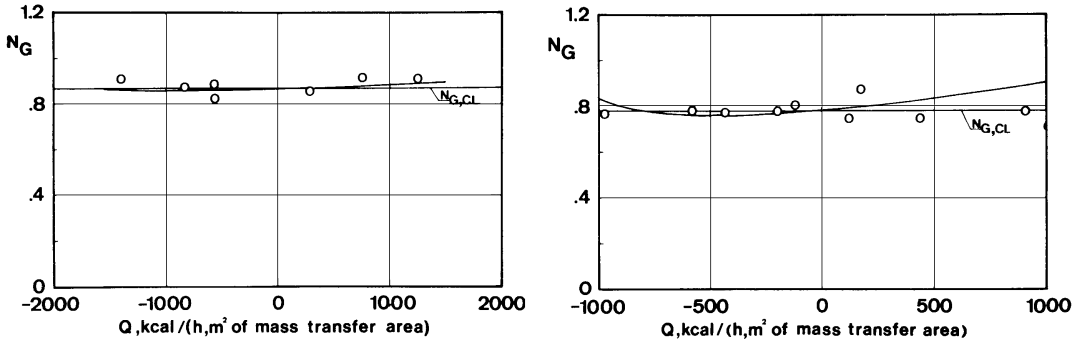

Fig. 1. Results of two runs of a previous study using a jacketed wetted-wall column [2]. Left (methanol–water): $\lambda_1/\lambda_2=0.840$, $K_G=0.566$ kmol/(m^2 h), $V_{in}=41.5$ kmol/h. Right (*n*-heptane–toluene): $\lambda_1/\lambda_2=0.959$, $K_G=0.139$ kmol/(m^2 h), $V_{in}=11.4$ kmol/h.

The effect of abnormally high deviation from equimolar countertransfer in binary distillation was studied in an earlier work [1,2]. The most important findings of that work will be recapitulated below.

It was shown theoretically, using film and penetration theories, that a favorable cancellation of heat effects due to highly unequal molar heats of vaporization or highly nonadiabatic operation can be anticipated. Based on this, it was shown computationally that, on a distillation column plate with perfect mixing of liquid and plug flow of vapor, the classical point efficiency based on equimolar countertransfer coincides quite accurately with the 'exact' point efficiency. The deviation from unity of the ratio of the point efficiency values appeared in the third decimal for a mixture with λ_1/λ_2 varying from 0.5 to 1.5 and for nonadiabatic operation with $Q/\bar{\lambda}K_G$ varying from -0.05 to $+0.05$, where Q is the heat flux entering or leaving the liquid through the wall and K_G is the overall mass transfer coefficient.

The striking result was verified experimentally using a laboratory-scale jacketed wetted-wall column, which permitted an extremely high heat flux through the column wall. The results of two runs are given in Fig. 1 in terms of the number of mass transfer units N_G as a function of the heat flux Q. The conclusions to be drawn are similar to those for the other two runs using the same mixtures: N_G is practically uninfluenced by Q, and the classical ($N_{G,CL}$) and the 'exact' model are equally powerful in explaining the experimental points within a wide range around the adiabatic or equimolar operating point. In fact, the deviation from adiabatic or equimolar operating conditions extended much further in the experiments than in the theoretical study. In terms of the parameter $Q/\bar{\lambda}K_G$, the range for methanol–water was from -0.3 to $+0.3$ and that for *n*-heptane–toluene from -0.9 to $+0.9$. The final conclusion was that the classical model of binary distillation based on equimolar countertransfer can be used safely as a rigorous method for most practical purposes to obtain vertical composition profiles in a column or mass transfer efficiencies based on the profiles. At the same time, it was noted that heat effects should not be ignored when calculating the molar flows.

There are peculiarities in multicomponent mass transfer which are not encountered with binary mixtures. For this reason, not all conclusions that apply to binary distillation can be expected to apply directly to a multicomponent case. The peculiarities are neatly explained by the Maxwell–Stefan theory of multicomponent mass transfer [3]. There is, however, no explanation to be found from the same theory for why the above conclusions for binary distillation could not apply to multicomponent distillation run in comparable circumstances. For this reason, the above studies of nonadiabatic binary distillation are here extended to apply to multicomponent reactive distillation where the deviation from equimolar countertransfer is caused by a considerable release (consumption) of heat of reaction. The reaction is restricted to take place in the reaction zone of a reactive distillation column at the surface of a solid catalyst which is in contact with the liquid but not with the vapor. To distinguish this important application from reactive distillation where the reaction takes place in the fluid phase without a solid catalyst, the term 'catalytic distillation' is used.

The specific aim of the paper is to examine the effect of heat of reaction on vertical composition profiles on the vapor side in a column section, where liquid can be assumed to be perfectly mixed, as on a single plate in a reaction zone. The validity of the striking result obtained earlier for binary distillation will then be judged for multicomponent catalytic distillation, and the chances to make significant advances in model solving on that basis will be evaluated.

2. Molar flux across the vapor–liquid interface

Consider the vapor–liquid interface on a plate in a reaction zone of a catalytic distillation column. Because the chemical reaction takes place at the catalyst surface which is in contact with the liquid only, the reaction and the vapor do not 'know' about each other. Only the state of the liquid has an effect on the rate and the extent of the reaction. The only reaction-related information that reaches the vapor is the state of the liquid at the vapor–liquid interface, i.e. its

composition and its excess need to release or consume heat to remain saturated.

To visualize the situation from the perspective of the vapor film in the case of an exothermic reaction, the vapor–liquid interface can be viewed as a permeable wall through which a steady flux of energy is being pushed in the form of latent heat of vapor due to the excess energy behind the 'wall'. On the vapor side, then the mass transfer is composed of diffusional fluxes of components driven by the concentration differences across the vapor film and a total (net) molar flux satisfying the excess need to transfer energy originating from the reaction. A corresponding visualization applies to an endothermic reaction as well.

The above description outlines roughly what is believed to happen behind the 'wall'. Vaporization and condensation are constrained to take place at the gas–liquid interface of the vapor bubbles entering the plate. With an exothermic reaction, for instance, the heat released at the solid surface — probably inside a catalyst particle — is thought to be transferred onto the outer surface of the catalyst particle and further through the body of liquid to the vapor–liquid interface, where evaporation takes place. In other words, no bubble formation at the solid surface or in the bulk of the liquid would occur. This implies that, in spite of some overheating of the liquid necessary for building a temperature gradient, there is fast enough heat transfer and a high enough nucleation barrier in the liquid to prevent any bulk boiling. While this mechanism may be questioned in the case of an extremely exothermic reaction, the experimental evidence from the earlier work strongly supports it. Neither bubble formation in the bulk of liquid nor mist formation in the bulk of vapor was observed in the extreme nonadiabatic conditions of the wetted-wall column made of glass [2].

Making the usual assumption that thermodynamic equilibrium applies at the vapor–liquid interface, it is possible to analyze mass transfer on the vapor side in terms of the total molar flux and the equilibrium composition at the interface with no direct reference to the chemical reaction or to the transfer phenomena on the liquid side. Consequently, the following analysis of multicomponent mass transfer in the vapor film applies with no regard whether the excess need of liquid at the vapor–liquid interface to release or consume heat refers to a chemical reaction, nonadiabatic operation, unequal molar heats of vaporization, or some other heat effects.

Total molar flux (n_t) has a central role in assessing heat effects on the molar fluxes of components (**n**). Its contribution is given by

$$\mathbf{n} = \mathbf{j} + n_t\mathbf{y} \tag{1}$$

where **j** is the diffusional flux vector and **y** is the vector of the molar fractions on the vapor side. The diffusional flux is obtained from the Maxwell–Stefan equations, which, according to the linearized theory of multicomponent mass transfer, simplify to Eq. (2) in the case of an ideal system,

$$\mathbf{j} = -c_t\mathbf{D}\frac{\mathrm{d}\mathbf{y}}{\mathrm{d}r} = -c_t\mathbf{B}^{-1}\frac{\mathrm{d}\mathbf{y}}{\mathrm{d}r} \tag{2}$$

Here the parameters c_t and **D** can be considered constant. **D** is obtained from **B**, whose composition-dependent elements are evaluated at some proper composition along the diffusion path (see e.g. [3]).

By transforming the variables $\mathbf{y} = \mathbf{P}\hat{\mathbf{y}}$, where **P** is the modal matrix of **D**, and by multiplying by $\mathbf{P}^{-1}$ from the left, Eqs. (1) and (2) yield, after division by n_t,

$$\frac{c_t}{n_t}\hat{\mathbf{D}}\frac{\mathrm{d}\hat{\mathbf{y}}}{\mathrm{d}r} = \hat{\mathbf{y}} - \hat{\boldsymbol{\varphi}} \tag{3}$$

which is a set of uncoupled differential equations in terms of pseudo-composition $\hat{y}_i$ and transformed flux ratios $\hat{\varphi}_i = \hat{n}_i/n_t$.[1]

The solution for pseudo-composition is formally identical with that for actual composition in binary mass transfer, yielding the following profile in the film:

$$\frac{\hat{y}_{i0} - \hat{y}_i(\eta)}{\hat{y}_{i0} - \hat{y}_{i\delta}} = \frac{\eta\exp\hat{\Psi}_i - 1}{\exp\hat{\Psi}_i - 1} \tag{4}$$

where

$$\hat{\Psi}_i = \frac{n_t l}{c_t\hat{D}_i} = \frac{n_t}{c_t\hat{k}_i} \tag{5}$$

$$\eta = \frac{r - r_0}{r_\delta - r_0} = \frac{r - r_0}{l} \tag{6}$$

In Eq. (5), the relationship $\mathbf{K}_\delta = \mathbf{D}_\delta/l$ has been applied, which follows from the definition of a low-flux mass transfer coefficient [3].

By differentiating Eq. (4) with respect to η, the gradient at the bulk end of the film (at η=1) is obtained, from which it follows that

$$\hat{\mathbf{j}}_\delta = c_t\hat{\mathbf{K}}_\delta^{\bullet}(\hat{\mathbf{y}}_0 - \hat{\mathbf{y}}_\delta) \tag{7}$$

$$\hat{\mathbf{K}}_\delta^{\bullet} = \hat{\mathbf{K}}_\delta\hat{\boldsymbol{\Xi}}_\delta \tag{8}$$

$$\hat{\boldsymbol{\Xi}}_\delta = \hat{\boldsymbol{\Psi}}_\delta\exp\hat{\boldsymbol{\Psi}}_\delta(\exp\hat{\boldsymbol{\Psi}}_\delta - \mathbf{I})^{-1} \tag{9}$$

$$\hat{\boldsymbol{\Psi}}_\delta = \frac{n_t}{c_t}\hat{\mathbf{K}}_\delta^{-1} \tag{10}$$

When the total molar flux (n_t) approaches zero, the eigenvalues of the correction matrix approach unity and the eigenvalues of the mass transfer coefficient matrix approach those prevailing in low-flux conditions.

While the exact solution of Maxwell–Stefan equations can be obtained for ideal gas mixtures, the approximate solution to be obtained by using the linearized theory has been shown to have an excellent accuracy compared to the exact

[1] The following unified notation has been adopted: $\hat{\mathbf{A}} = [\hat{A}_i] = \mathbf{P}^{-1}\mathbf{A}\mathbf{P}$, $\hat{\mathbf{q}} = \mathbf{P}^{-1}\mathbf{q}$, where $\hat{\mathbf{A}}$ stands for diagonal matrix of eigenvalues $\hat{A}_i$ and $\hat{\mathbf{q}}$ stands for a vector of transformed quantities, or pseudo-quantities, $\hat{q}_i$. As usual, $\mathbf{P}^{-1}$ is the inverse of **P** and $\exp\mathbf{A}$ is an exponential function with **A** as the exponent.

solution by several authors (see e.g. [3]). It has been pointed out by Burghardt and Warmuzinski [4] that the linearized theory may lead to a certain error in some cases, but in the light of experimental results, the risk of such an error is insignificant. For engineering purposes, the linearized theory is believed to be the most important method for solving multicomponent diffusion problems [3]. In this work, the use of the linearized theory permits conclusions about the heat effects on the composition profiles along the height of the distillation column without a need to specify the mixture, as will be shown in the next section.

3. Balance equations and associated assumptions

In this and the following chapter, a set of assumptions will be made as part of the model building. They will be specified as the modeling proceeds. To help the reader, each assumption is identified with a lower case letter in parentheses. The assumptions will be summarized in Section 6.

Consider a catalytic distillation column section, where (a) liquid can be assumed to be perfectly mixed, such as a single plate in the reaction zone of a column, as depicted in Fig. 2. Component balance around the body of liquid is

$$L_{\text{out}}\mathbf{x}_{\text{out}} = L_{\text{in}}\mathbf{x}_{\text{in}} + \boldsymbol{\alpha}R - \mathbf{n}aAh_{\text{t}} \tag{11}$$

where R is the extent of reaction. In accordance with the aim of this study, it will be assumed that (b) the reaction is fast enough to achieve chemical equilibrium, while mass transfer across the vapor–liquid interface is the rate-limiting step. This permits an estimate of the upper limit of the heat released (consumed).

Total molar balance for the liquid is

$$L_{\text{out}} = L_{\text{in}} + \sum \alpha_i R - n_{\text{t}}aAh_{\text{t}} \tag{12}$$

By assuming that (c) the enthalpy flow associated with liquid entering and leaving the plate is negligible compared to the enthalpy flows through the catalyst–liquid and gas–liquid interfaces, the enthalpy balance for the liquid simplifies to

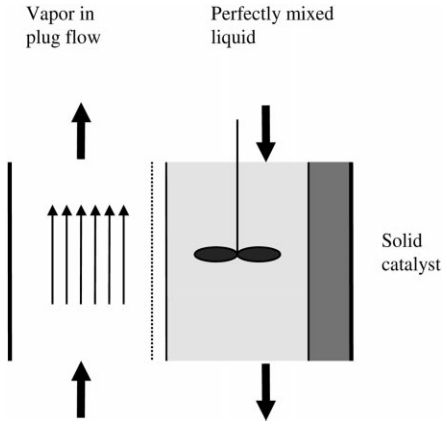

Fig. 2. Column section in the reactive zone.

$$(-\Delta H_{\text{R}})R = \bar{\lambda}n_{\text{t}}aAh_{\text{t}} \tag{13}$$

In Eq. (13) the molar heats of vaporization of components are replaced by an average $\bar{\lambda}$. This is based on the assumption that (d) the net enthalpy flow through the gas–liquid interface caused by unequal molar heats of vaporization is negligible compared to the term on the right-hand side of Eq. (13), i.e. the enthalpy flow caused by the heat of reaction. The contribution of heat conduction across the interface driven by a temperature gradient is neglected as usually. It is now possible to estimate the upper limit of the total molar flow across the interface as follows:

$$n_{\text{t}}aAh_{\text{t}} = \xi R \tag{14}$$

where $\xi = -\Delta H_{\text{R}}/\bar{\lambda}$ is the 'heat utilization factor' introduced by Sundmacher et al. [5].

In accordance with the normal practice, it is assumed that (e) vapor remains axially unmixed or in plug flow, as it rises as bubbles through the liquid. Thus, the following component and total molar balances are obtained for a differential slice of vapor:

$$\mathrm{d}V = n_{\text{t}}aA\,\mathrm{d}h \tag{15}$$

$$\mathrm{d}(\mathbf{y}V) = \mathbf{n}aA\,\mathrm{d}h \tag{16}$$

Substituting Eqs. (1) and (15) into Eq. (16), the terms explicitly including n_{t} cancel out, leaving simply

$$V\,\mathrm{d}\mathbf{y} = \mathbf{j}aA\,\mathrm{d}h \tag{17}$$

(For notational simplicity, the subscript δ has been dropped here, as will be done later whenever reference is made to the vapor bulk conditions.) The fact that the term n_{t} does not appear in Eq. (17), while it appears in Eq. (15), makes one expect that the profile of $\mathbf{y}$ is much less affected by n_{t} than the profile of V. In fact, Eq. (17) is structurally identical to the component balance to be obtained for truly equimolar countertransfer (n_{t}=0). The difference is that Eq. (17) still includes the contribution of n_{t} implicitly in the terms on both sides (in V and $\mathbf{j}$). Inspection of how this contribution affects the profile of $\mathbf{y}$ when compared to the truly equimolar case is possible by making the dependence explicit.

With a nonzero n_{t}, V varies with h as obtained from Eq. (15). The dependence of $\mathbf{j}$ on n_{t} is obtained using Eqs. (7)–(10). While the ultimate aim is to determine the contribution quantitatively, straightforward qualitative reasoning is possible if Eq. (17) is first transformed to the uncoupled form

$$V\frac{\mathrm{d}\hat{\mathbf{y}}}{\mathrm{d}h} = \hat{\mathbf{j}}aA = c_{\text{t}}aA\hat{\mathbf{K}}^{\bullet}(\hat{\mathbf{y}}_0 - \hat{\mathbf{y}}) \tag{18}$$

For a thermodynamically stable fluid, the matrix $\mathbf{D}$ is positive definite [6], which means that all its eigenvalues are real and positive. Thus, when n_{t} is positive, which means that V increases with column height, the eigenvalues $\hat{\Psi}_i$ of the dimensionless rate factor matrix $\hat{\boldsymbol{\Psi}}$ are positive. This means,

in turn, that the eigenvalues $\hat{\Xi}_i$ of the correction matrix $\hat{\Xi}$ are larger than unity, making the eigenvalues of the mass transfer coefficient matrix, which appear on the right-hand side of Eq. (18), larger than those in low-flux conditions. Thus, a deviation of n_t from zero in a positive (negative) direction makes *both* sides of Eq. (18) increase (decrease), and the influence of even highly nonzero n_t on the profile of y may be expected to be slight. This result would be in agreement with the previous findings for binary distillation. If the cancellation were close enough to perfect, it would make it possible to integrate Eq. (17) by keeping V constant and replacing the correction matrix in $\hat{\mathbf{j}}$ by the identity matrix. This would mean a major simplification when solving the balance equations for vapor and liquid compositions.

4. Cancellation of heat effects

The mass and energy balances for a catalytic distillation column section make up a set of coupled algebraic and differential equations. The coupling between the phases is via the molar fluxes across the interface and the balances for the plate and the adjacent column sections above and below. In an iterative solution of this set of equations, the differential mass balances for vapor, Eqs. (15) and (17), are integrated by keeping two coupling variables, $\mathbf{y}_0$ and n_t, fixed within each iteration cycle. Analytic integration is desirable to warrant general conclusions concerning the effect of n_t on the solution. For that, a few additional assumptions will be necessary.

For purely mathematical simplicity, it is assumed that (f) the mass and heat transfer resistances on the liquid side are negligible. (Recall that the analysis in Section 2 of multicomponent mass transfer in the vapor film was independent of the assumptions concerning transfer phenomena on the liquid side.) This is equal to assuming that the liquid side molar fractions at the interface ($\mathbf{x}_0$) are equal to those prevailing in the bulk of liquid (which are equal to $\mathbf{x}_{out}$, because liquid is assumed to be perfectly mixed). Since thermodynamic equilibrium prevails at the interface, the vapor phase molar fractions at the interface end of the vapor film ($\mathbf{y}_0$) are also independent of section height. Although it is often acceptable to ignore the resistance in the liquid phase in distillation, the intention here is only to avoid excessively awkward equations whenever this appears plausible from the point of view of reasoning about the cancellation of heat effects. The resulting spatial uniformity at the interface of the excess need of liquid to release (consume) heat makes the total flux n_t across the interface constant in the integration along the section height. This makes it possible to integrate Eq. (15) analytically, giving

$$V = V_{in}[1 + \hat{\Psi}_i \hat{N}_i(h)] \tag{19}$$

where $\hat{N}_i(h)$ is an eigenvalue of the number of mass transfer units matrix

$$\hat{N}_i(h) = c_t a A h V_{in}^{-1} \hat{k}_i \tag{20}$$

Substituting Eq. (19) for V in Eq. (18) results in the following equation:

$$[1 + \hat{\Psi}_i \hat{N}_i(h)] \frac{d\hat{y}_i}{dh} = \frac{d\hat{N}_i}{dh} \hat{\Xi}_i (\hat{y}_{i,0} - \hat{y}_i) \tag{21}$$

Eq. (20) implies that

$$\frac{d\hat{N}_i}{dh} = c_t a A V_{in}^{-1} \hat{k}_i \tag{22}$$

which is based on the assumption that (g) mass transfer coefficients do not vary with h in the column section. While this assumption is normally valid in multicomponent distillation, its goodness was not studied in this work. It is believed, instead, that any error introduced by this assumption can safely be taken into account when necessary by estimating the composition-dependent elements of **B** in Eq. (2) at some average mole fraction of each component along the height of the column section.

Upon integration over the height, Eq. (21) yields the following generic pseudo-composition profile in the bulk of vapor:

$$\frac{\hat{y}_{i,0} - \hat{y}_i(h)}{\hat{y}_{i,0} - \hat{y}_{i,in}} = [1 + \hat{\Psi}_i \hat{N}_i(h)]^{-\hat{\Xi}_i/\hat{\Psi}_i} = \hat{f}_i(h) \tag{23}$$

as a function of two parameters only ($\hat{\Psi}_i$ and $\hat{N}_i$).

If the cancellation of the thermal effects happened to be perfect, Eq. (21) would simplify to that prevailing in the truly countercurrent mass transfer

$$\frac{d\hat{y}_i}{dh} = \frac{d\hat{N}_i}{dh} (\hat{y}_{i,0} - \hat{y}_i) \tag{24}$$

with the solution

$$\frac{\hat{y}_{i,0} - \hat{y}_i(h)}{\hat{y}_{i,0} - \hat{y}_{i,in}} = \exp[\hat{N}_i(h)] = \hat{g}_i(h) \tag{25}$$

To compare the two pseudo-composition profiles, as given by Eqs. (23) and (25), and to make general conclusions about the cancellation, the eigenvalues of the rate factor matrix ($\hat{\Psi}_i$) and those of the number of mass transfer units matrix ($\hat{N}_i$) need to be given proper numerical values. While the two parameters may vary over fairly wide ranges, the upper limit of the absolute magnitude of their product is bound by the quantity ξR, because (by definition)

$$\hat{\Psi}_i \hat{N}_i(h_t) = \frac{n_t a A h_t}{V_{in}} \tag{26}$$

where i may refer to any component. The right-hand side is the ratio of the total molar flow across the interface and the incoming vapor molar flow. The dimensionless parameter $\hat{\Psi}_i \hat{N}_i(h_t)$ can thus be taken as a measure of nonequimolarity. It may assume both positive and negative values with zero referring to equimolarity. A feasible maximum absolute value for $\hat{\Psi}_i \hat{N}_i(h_t)$ must obviously be less than 1.

The generic pseudo-composition profiles for the case of exothermic catalytic distillation are compared graphically

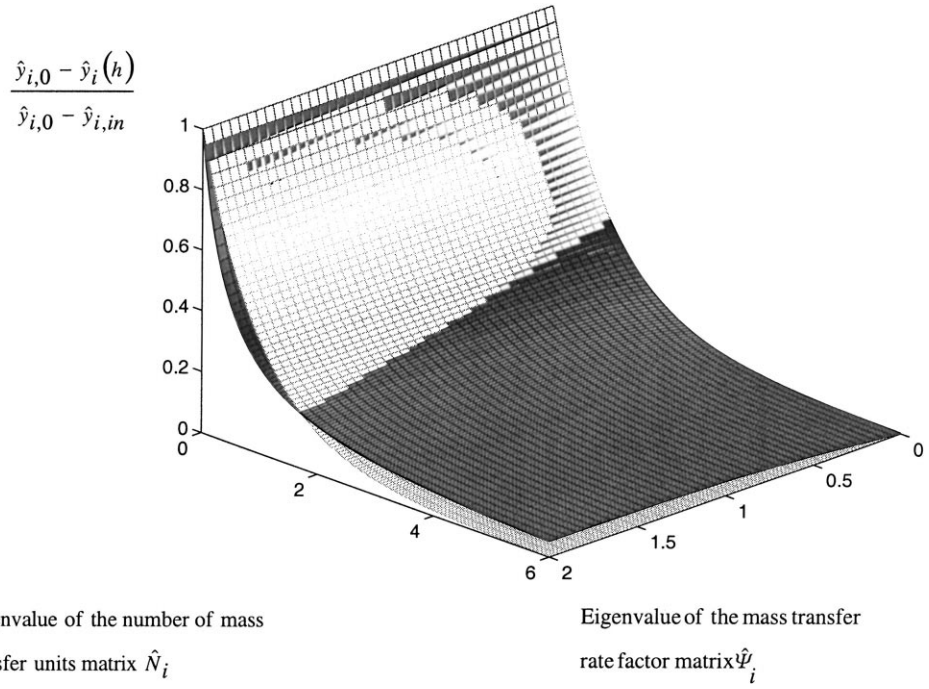

Fig. 3. The dimensionless pseudo-component profiles in vapor phase as a function of $\hat{\Psi}_i$ and $\hat{N}_i$ (dark surface refers to $\hat{f}_i$).

in Figs. 3 and 4 by letting $\hat{N}_i(h)$ to vary between 0 and 6 and $\hat{\Psi}_i$ between 0 and 2. The negative region of $\hat{\Psi}_i$, corresponding to an endothermic reaction, has less interest and is left outside the numerical study. The error $(\hat{f}_i - \hat{g}_i)$, introduced by neglecting the heat effect completely, is shown as the vertical distance between the two surfaces in Fig. 3. The difference is depicted separately in Fig. 4. It should be noted, when inspecting the figures, that only those regions on the surfaces are feasible where the product of the two parameters is less than the feasible maximum. The feasible region in Fig. 4 is the one which remains between the two horizontal coordinate axes and the hyperbola $\hat{\Psi}_i \hat{N}_i(h_t) = 1$.

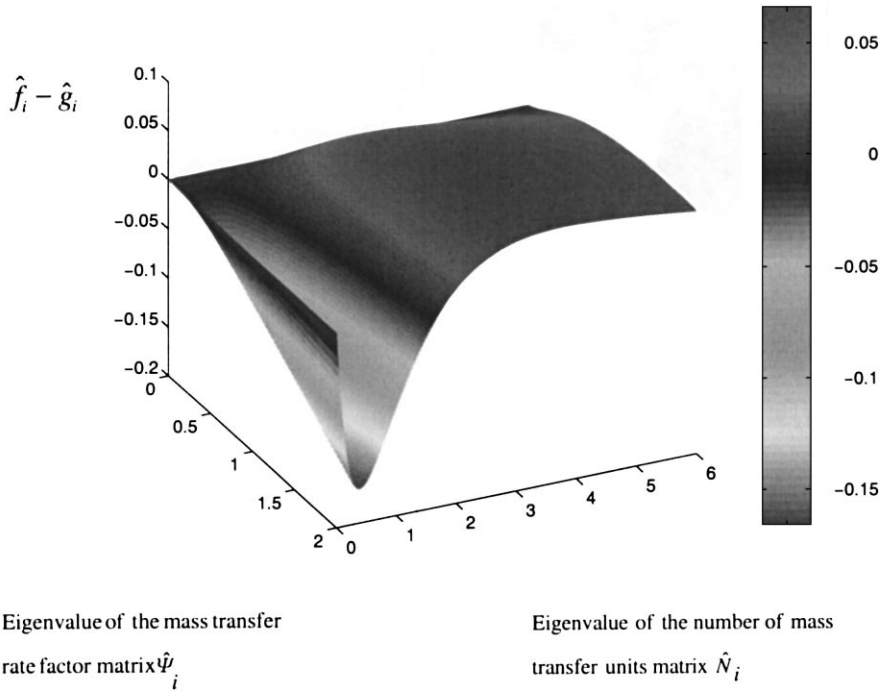

Fig. 4. The error $(\hat{f}_i - \hat{g}_i)$ introduced by neglecting the heat effect totally.

The conclusions to be drawn from the comparison are parallel to those obtained earlier for binary distillation in highly nonadiabatic conditions. Quite obviously, cancellation of the effects of the reaction-induced total flux across the interface does take place. The peculiar shape of the error surface in Fig. 4 enables one to make the following specific conclusions.

The error introduced into the pseudo-composition profile on the vapor side becomes negligible when the rate of interfacial mass transfer increases. This is because the factors that make $\hat{N}_i(h_t)$ high make the corresponding $\hat{\Psi}_i$ low. These factors, which originate from plate hydrodynamics, are the thickness of the vapor film (l) and the specific mass transfer area (a). (Recall that $\hat{N}_i$ is proportional to a/l and $\hat{\Psi}_i$ to l.) To visualize the error, assume, for instance, that $\hat{N}_i(h_t)$ equals 5.0, which can be taken to correspond to a plate not far from the theoretical. (Note that $\hat{N}_i(h_t) = 5.0$ corresponds to a point efficiency equal to 99.3%.) Then $\hat{\Psi}_i$ should be less than 0.2. The trajectory of the error on the surface in Fig. 4 when integrating from 0 to h_t is inside a band limited by $\hat{N}_i(h) = 0, \ldots, 5$, and $\hat{\Psi}_i = 0, \ldots, 0.2$. In this whole region, the deviation of the surface from zero is very small. Thus, if the plate is close to a theoretical plate, the differential composition balance based on equimolar countertransfer, Eq. (24), can be used safely to characterize the whole composition profile in the vapor phase.

If mass transfer is only moderate compared to the rate of heat generation, say, $\hat{N}_i(h_t) = 1.0$, then $\hat{\Psi}_i < 1$ and the error trajectory is within the band limited by $\hat{N}_i(h_t) = 0, \ldots, 1$ and $\hat{\Psi}_i = 0, \ldots, 1$. It can be seen that if $\hat{\Psi}_i$ is close to the upper limit, a negative error is introduced into the lower region of the pseudo-composition profile. This region coincides with the valley shown in Fig. 4. The error in the pseudo-composition of the outflowing vapor (at $h{=}h_t$), however, remains small. Thus, if a real plate is characterized by a point efficiency higher than, say, 60%, Eq. (24) can be used safely to solve the composition of the outflowing vapor in any conditions. It should be noted, however, that the upper limit corresponds to conditions where the total molar flow across the vapor–liquid interface is equally large as the vapor flow entering the plate. If a more realistic situation is assumed, say, the former is 10% of the latter, then $\hat{\Psi}_i = 0.1$ and the error is negligible along the whole trajectory.

If, for some reason, a plate in the reaction zone is very inefficient with respect to mass transfer ($\hat{N}_i(h_t) < 1.0$), it may happen that the error in the pseudo-composition of the outflowing vapor also coincides with the valley on the error surface. If the extent of reaction and the associated release of heat are simultaneously high ($\hat{\Psi}_i > 1.0$), the plate operates at the deep end of the valley and the error may be intolerable. Assume, for instance, that with $\hat{N}_i(h_t) = 0.5$ the value of $\hat{\Psi}_i$ is as high as 2.0. Then the error at $h{=}h_t$ would be -0.15, as can be readily seen from Fig. 4. By the same argument as above, a more probable value would be $\hat{\Psi}_i = 0.2$, whereby the error becomes tolerable.

5. Example

In order to make the comparison discussed above in terms of pseudo-compositions more concrete, the cancellation of heat effects will be illustrated in terms of actual compositions by inverting Eqs. (23) and (25). For this purpose, production of methyl *tert*-butyl ether (MTBE) by catalytic distillation was chosen as the case.

Consider a plate in the reaction zone of an MTBE catalytic distillation column. The liquid and vapor on the plate are mixtures composed of four components: isobutene (ISO-B), methanol (MEOH), MTBE, and butane (N-BUT). The following exothermic chemical reaction takes place at the surface of a solid catalyst in contact with the liquid: MEOH+ISO-B↔MTBE.

The composition profiles on the vapor side in terms of the actual mole fractions of the four components are obtained by inverting the pseudo-component profiles, Eqs. (23) and (25), as follows:

$$\mathbf{y}(h) = \mathbf{y}_0 - \mathbf{P}\hat{\mathbf{F}}(h)\mathbf{P}^{-1}(\mathbf{y}_0 - \mathbf{y}_{in}) \tag{27}$$

$$\mathbf{y}(h) = \mathbf{y}_0 - \mathbf{P}\hat{\mathbf{G}}(h)\mathbf{P}^{-1}(\mathbf{y}_0 - \mathbf{y}_{in}) \tag{28}$$

where $\hat{\mathbf{F}}$ and $\hat{\mathbf{G}}$ are diagonal matrices,

$$\hat{\mathbf{F}} = [\hat{f}_i] \quad \text{and} \quad \hat{\mathbf{G}} = [\hat{g}_i] \tag{29}$$

The inversion implies a computation procedure with a set of initial data. A comparison of the compositions of the vapor leaving the plate, as obtained from Eqs. (27) and (28), is meaningful even when the flow rates and compositions of the liquid and vapor entering and leaving the plate are not numerically coupled by the balances around the column sections above and below. That is why, instead of solving the whole column, properly chosen values of L_{in}, $\mathbf{x}_{in}$, V_{in}, and $\mathbf{y}_{in}$ were taken as input data. In addition, to avoid the excess computational burden due to the inclusion of the reaction mechanism and kinetics, it was assumed (as in Section 3) that the reaction at the catalyst surface is fast enough to advance to equilibrium. Then the composition of the saturated liquid in contact with the catalyst is always the reaction equilibrium composition $\mathbf{x}_{eq}$. This composition can be evaluated iteratively from the temperature dependence of the equilibrium constant, starting from the composition of the saturated liquid entering the plate ($\mathbf{x}_{in}$). An estimate of the extent of reaction R can then be obtained by solving the liquid side molar balances with the vapor–liquid interface temporarily closed ($\mathbf{n}{=}0$, $n_t{=}0$) and by substituting $\mathbf{x}_{eq}$ for $\mathbf{x}_{out}$. One obtains, in terms of MTBE,

$$R \approx L_{in}\frac{x_{eq,MTBE} - x_{in,MTBE}}{1 + x_{eq,MTBE}} \tag{30}$$

The temperature dependence of the equilibrium constant used is the one given by Rehfinger and Hoffmann [7]. For the 'heat utilization factor', a reasonable value $\xi{=}1.5$ was obtained from [5] to represent a typical situation in the commercial MTBE catalytic distillation columns. An estimate

of the total molar flow across the interface is then obtained from Eq. (14), which yields the following overall changes in the flows across the plate:

$$\Delta L = L_{\text{in}} - L_{\text{out}} = \left(\sum \alpha_i - \xi\right) R = -2.5R \tag{31}$$

$$\Delta V = V_{\text{in}} - V_{\text{out}} = \xi R = 1.5R \tag{32}$$

The phase equilibrium relationship for obtaining $\mathbf{y}_0$ was fixed by assuming an ideal vapor phase and by using Wilson's equation for the liquid phase. While the liquid composition at the interface $\mathbf{x}_0$=$\mathbf{x}_{\text{out}}$ does not have to be equal to $\mathbf{x}_{\text{eq}}$, because there may be a concentration gradient both within the pores of the catalyst and between the outer surface of the catalyst and the bulk of liquid, the first guess for $\mathbf{y}_0$ is obtained by assuming that $\mathbf{x}_0$=$\mathbf{x}_{\text{eq}}$.

The binary diffusion coefficients, used to construct the Fick matrix **D**, were evaluated in terms of the Fuller correlation (see e.g. [3]). The elements of **D** were computed on each iteration cycle at the average composition of vapor defined as follows:

$$\mathbf{y}_{\text{av}} = \tfrac{1}{2}(\mathbf{y}_{\text{in}} + \mathbf{y}_{\text{out}}) \tag{33}$$

Eqs. (27) and (28) were evaluated iteratively by forcing $\mathbf{x}_{\text{out}}$ to satisfy the component balance around the plate:

$$L_{\text{out}}\mathbf{x}_{\text{out}} = L_{\text{in}}\mathbf{x}_{\text{in}} + \alpha R + V_{\text{out}}\mathbf{y}_{\text{out}} - V_{\text{in}}\mathbf{y}_{\text{in}} \tag{34}$$

which means that $\mathbf{x}_{\text{out}}$ ultimately deviates from $\mathbf{x}_{\text{eq}}$. The effect of this deviation on the extent of reaction (R) was not included, because it is rather the order of magnitude of R that is of interest in this context. The deviation is small when mass transfer efficiency is low, and with higher mass transfer rates, when the extent of reaction is subject to more influence, the effect of R on the composition profiles on the vapor side is known to be smaller.

The output compositions of each phase were computed for the two sets of input compositions given in Table 1. For both sets, the eigenvalue $\hat{\Psi}_{\text{ISO-B}}$ of the mass transfer rate factor matrix was varied between 2.0 and 0.1. The higher value implies a low mass transfer efficiency and was chosen only to force the solution into the unsafe region of the error surface. The values of $\hat{\Psi}_i$ for the rest of the components follow from $\hat{\Psi}_{\text{ISO-B}}$ on the strength of the assumption, inherent to the film theory, that film thickness is the same for each component. The product $\hat{\Psi}_i \hat{N}_i(h_{\text{t}})$ is independent of the component, as shown in Eq. (26), and is constant for each set of input compositions. It is obtained from

$$\hat{\Psi}_i \hat{N}_i(h_{\text{t}}) = \xi \left(\frac{L_{\text{in}}}{V_{\text{in}}}\right) \frac{x_{\text{eq,MTBE}} - x_{\text{in,MTBE}}}{1 + x_{\text{eq,MTBE}}} \tag{35}$$

which is a combination of Eqs. (14), (26) and (30). Using $L_{\text{in}}/V_{\text{in}}$=1, the two levels of the product $\hat{\Psi}_i \hat{N}_i(h_{\text{t}})$ are 0.2 and 0.4. The resulting variation of $\hat{N}_i(h_{\text{t}})$ covers a wide region on the error surface in Fig. 4, including the valley.

The results, which are given in Table 1 in terms of the actual molar fractions of the vapor and liquid streams leaving the plate, fully support the conclusions drawn from the pseudo-component profiles of Figs. 3 and 4.

On a plate with a very low mass transfer efficiency corresponding to the region of $\hat{N}_i(h_{\text{t}})$ around 0.3, the error in the computed molar fractions appears in the second significant digit. For components in the vapor phase with concentrations decreasing with height (ISO-B, MEOH and MTBE), the molar fractions in the output, as given by the simple model, are somewhat too low on such a plate. Correspondingly, the vapor output concentration of N-BUT is too high. These deviations are in good agreement with what can be predicted from Fig. 4. In the liquid output, the deviations are naturally opposite in direction. The error may be intolerable, but limited to conditions unlikely to be encountered in normal practice.

At higher efficiencies further away from the valley, the error is in the third significant digit or less and can be regarded as insignificant.

6. Discussion

This paper aims to take a meaningful step forward in the design methodology of reactive distillation by reducing the degree of interdependence between the chemical reaction and the interphase mass transfer without a simultaneous loss of realism in the model for predicting vertical composition profiles in a column. The earlier findings for highly nonequimolar binary distillation are shown to be valid in multicomponent distillation in comparable circumstances, i.e. with a highly exothermic (endothermic) heterogeneously catalyzed reaction on the liquid side. As a result, nonequimolarity can be safely ignored in most practical cases of multicomponent catalytic distillation when computing bulk compositions on a plate in the reaction zone of a column. The origin of nonequimolarity is attributed primarily not only to the heat of reaction, but also to conditions which may be present even in ordinary distillation like unequal heats of vaporization of components and nonadiabatic operation. The result should not, however, be interpreted to mean that such effects could be ignored when computing molar flows in a column. The practical benefit will be gained by avoiding the tedious algorithms developed for the Maxwell–Stefan equations for fluxes across a vapor–liquid interface in a nonequimolar case, when solving composition profiles.The following simplifying assumptions were needed to arrive at the conclusion: (a) liquid can be assumed to be perfectly mixed; (b) the reaction is fast enough to achieve chemical equilibrium; the enthalpy flow associated with the liquid entering and leaving the plate is negligible compared to the enthalpy flows through the catalyst–liquid and gas–liquid interfaces; (c) the net enthalpy flow through the gas–liquid interface caused by unequal molar heats of vaporization is negligible compared to the term on the right-hand side of Eq. (13), i.e. the enthalpy flow caused by the heat of reaction; (d) vapor remains axially unmixed, or in plug flow,

Table 1
Compositions of vapor and liquid departing the column section $x_{out,i}$ and $y_{out,i}$ with two different input flow compositions $x_{in,i}$ and $y_{in,i}$

i	$x_{in,i}$	$y_{in,i}$	$\hat{\Psi}_i$	$\hat{N}_i$	$x_{out,i}$ (including heat effects)	$x_{out,i}$ (ignoring heat effects)	$y_{out,i}$ (including heat effects)	$y_{out,i}$ (ignoring heat effects)
ISO-B	0.150	0.050	2.000	0.102	0.015	0.012	0.045	0.046
MEOH	0.150	0.050	1.015	0.202	0.015	0.013	0.045	0.046
MTBE	0.050	0.200	1.602	0.128	0.269	0.246	0.173	0.186
N-BUT	0.650	0.700			0.701	0.729	0.737	0.722
ISO-B	0.150	0.050	1.000	0.205	0.017	0.015	0.043	0.044
MEOH	0.150	0.050	0.588	0.348	0.017	0.017	0.043	0.044
MTBE	0.050	0.200	0.801	0.255	0.283	0.267	0.166	0.175
N-BUT	0.650	0.700			0.683	0.701	0.747	0.737
ISO-B	0.150	0.050	0.500	0.409	0.019	0.019	0.042	0.043
MEOH	0.150	0.050	0.254	0.805	0.020	0.020	0.042	0.042
MTBE	0.050	0.200	0.401	0.511	0.307	0.299	0.153	0.157
N-BUT	0.650	0.700			0.654	0.662	0.763	0.758
ISO-B	0.150	0.050	0.100	2.046	0.022	0.022	0.041	0.041
MEOH	0.150	0.050	0.051	4.020	0.023	0.023	0.040	0.040
MTBE	0.050	0.200	0.080	2.551	0.378	0.380	0.114	0.113
N-BUT	0.650	0.700			0.577	0.575	0.805	0.806
ISO-B	0.300	0.100	2.000	0.205	0.021	0.016	0.086	0.087
MEOH	0.300	0.100	1.035	0.395	0.031	0.028	0.083	0.084
MTBE	0.050	0.500	1.618	0.253	0.668	0.586	0.433	0.451
N-BUT	0.350	0.300			0.280	0.370	0.398	0.378
ISO-B	0.300	0.100	1.000	0.409	0.023	0.022	0.085	0.085
MEOH	0.300	0.100	0.519	0.788	0.036	0.036	0.082	0.082
MTBE	0.050	0.500	0.810	0.505	0.695	0.668	0.427	0.433
N-BUT	0.350	0.300			0.246	0.274	0.406	0.400
ISO-B	0.300	0.100	0.500	0.818	0.024	0.024	0.085	0.085
MEOH	0.300	0.100	0.260	1.574	0.039	0.040	0.081	0.081
MTBE	0.050	0.500	0.406	1.009	0.727	0.723	0.420	0.421
N-BUT	0.350	0.300			0.210	0.213	0.414	0.413
ISO-B	0.300	0.100	0.100	4.091	0.025	0.025	0.085	0.085
MEOH	0.300	0.100	0.052	7.852	0.040	0.040	0.081	0.081
MTBE	0.050	0.500	0.081	5.038	0.765	0.765	0.411	0.411
N-BUT	0.350	0.300			0.170	0.170	0.423	0.423

as it rises as bubbles through the liquid; (e) mass and heat transfer resistances on the liquid side are negligible; (f) mass transfer coefficients do not vary with h in the column section.

Each assumption given above is common in the domain literature and can hence be regarded as reasonable. Here, these assumptions serve only to keep the mathematics simple. It is argued that each of them can be relaxed without violating the main conclusion that a favorable cancellation of heat effects occurs. The question that may be raised concerns the conditions where heat effects can be assumed to be *safely* ignored and the extent to which such a statement is dependent on the assumptions made.

Because the aim was to arrive at a general conclusion, the conditions need to be specified in terms of the pair of dimensionless parameters ($\hat{\Psi}_i$, $\hat{N}_i$). These are established parameters of the domain and have nothing to do with the assumptions. The parameters are defined by Eqs. (5) and (20). Their product, which can be used as a measure of nonequimolarity, is also given by Eq. (26). It is not quite straightforward to translate the conditions characterized by two dimensionless figures into a set of values of measurable parameters or vice versa. This is the price that has to be paid for a generic formulation. However, the product $\hat{\Psi}_i \hat{N}_i$ has a clear physical interpretation as the ratio of the total molar flow across the vapor–liquid interface to the vapor flow entering the plate and can be assessed based on that. (Recall that its value can be positive or negative.)

Another difficulty in specifying safe or unsafe range of conditions at the general level is the uncertainty concerning the purpose of using the model. What is an acceptable error for some purposes may not be that for some other purposes. However, by specifying — in terms of the two parameters — a region of conditions believed to represent the 'most practical cases of multicomponent catalytic distillation', it is easy to conclude, as shown in Fig. 4, that the error obviously remains acceptable 'for most practical purposes'. What cannot be seen from Fig. 4, however, is whether the relaxation of some of the assumptions would change the shape of the surface to the extent that the statement is violated and the acceptable region should be revised. Without aiming to prove

that this is not the case, it is suggested that Fig. 4 is accepted, as the first hypothesis, as the generic representation of the error introduced by ignoring heat effects, not skewed by the assumptions made. After this, one may try to disprove the hypothesis by relaxing the assumptions one by one and by checking whether a violation occurs. Such a test, however, implies efforts ranging from reasoning to simulation or experiments and is beyond the scope of this paper.

If Fig. 4 is accepted as the generic representation of the difference between dimensionless composition profiles including and ignoring the heat effects (constrained to positive values of $\hat{\Psi}_i$), the discussion in Section 4 concerning safe and unsafe regions applies as generic guidance. Especially, it is easy to specify a definitely unsafe region, where heat effects should not be neglected. This region, as discussed in Section 4, is the deep end of the valley in Fig. 4 and corresponds to very low mass transfer efficiency and a simultaneous huge release of heat of reaction, conditions not to be encountered in normal practice.

7. Nomenclature

a	interfacial area per unit volume of dispersion (m^2/m^3)
A	column cross-sectional area or active bubbling area (m^2)
B	matrix of Maxwell–Stefan diffusivities (s/m^2)
c_t	density of vapor mixture (mol/m^3)
$\mathbf{D}$	matrix of Fick diffusion coefficients (m^2/s)
$\hat{\mathbf{D}}$	eigenvalue matrix of $\mathbf{D}$
$\hat{D}_i$	ith eigenvalue of $\mathbf{D}$
h	vertical coordinate of a column section (m)
h_t	total height of a column section (m)
ΔH_R	heat of reaction (J/mol)
$\mathbf{I}$	identity matrix
$\mathbf{j}$	molar diffusion flux vector ($mol/m^2\,s$)
$\hat{\mathbf{j}}$	transformed molar diffusion flux vector ($mol/m^2\,s$)
$\hat{k}_i$	ith eigenvalue of the mass transfer coefficient matrix (m/s)
K_G	overall mass transfer coefficient ($kmol/m^2\,h$)
$\hat{\mathbf{K}}_\delta$	diagonalized mass transfer coefficient matrix (m/s)
l	diffusion path length or film thickness (m)
L	liquid flow in a column (mol/s)
ΔL	total change of the liquid flow in a column section (mol/s)
$\mathbf{n}$	vector of molar fluxes ($mol/m^2\,s$)
$\hat{n}_i$	ith transformed molar flux ($mol/m^2\,s$)
n_t	total molar flux ($mol/m^2\,s$)
$\hat{N}_i$	ith eigenvalue of the number of mass transfer unit matrix
$\mathbf{P}$	modal matrix of $\mathbf{D}$
Q	heat flux ($kcal/m^2\,h$)
r	diffusion path coordinate (m)
R	extent of reaction (mol/s)
V	vapor flow in a column section (mol/s)
ΔV	total change of the vapor flow in a column section (mol/s)
$\mathbf{x}$	vector of liquid molar fractions
$\hat{\mathbf{x}}$	vector of liquid pseudo-molar fractions
$\mathbf{y}$	vector of vapor molar fractions
$\hat{\mathbf{y}}$	vector of vapor pseudo-molar fractions

Greek letters

α	vector of stoichiometric coefficients
η	dimensionless distance along diffusion path
λ	molar heat of vaporization (J/mol)
$\bar{\lambda}$	average molar heat of vaporization (J/mol)
ξ	heat utilization factor
$\hat{\boldsymbol{\Xi}}_\delta$	diagonalized high-flux correction matrix
$\hat{\Xi}_i$	ith eigenvalue of the high-flux correction matrix
$\hat{\boldsymbol{\varphi}}$	vector of transformed flux ratios
$\hat{\varphi}_i$	ith transformed flux ratio
$\hat{\boldsymbol{\Psi}}_\delta$	diagonalized rate factor matrix
$\hat{\Psi}_i$	ith eigenvalue of the mass transfer rate factor matrix

Subscripts

i	component i
0	at the vapor–liquid interface
δ	at the bulk end of the vapor film
in	into a column section
out	out of a column section
eq	reaction equilibrium

References

[1] V.J. Pohjola, O. Smigelschi, Mass transfer in binary distillation with unequal molar fluxes of components: theory, Kemian Teollisuus 30 (1973) 5–9.
[2] O. Smigelschi, R.O. Riekko, V.J. Pohjola, Mass transfer in binary distillation with unequal molar fluxes of components: experiment on a wetted-wall column, Kemian Teollisuus 30 (1973) 63–66.
[3] R. Taylor, R. Krishna, Multicomponent Mass Transfer, Wiley, New York, 1993.
[4] A. Burghardt, K. Warmuzinski, Diffusional methods of calculation for multicomponent systems in rectification columns. I. Models of equimolar and nonequimolar mass transfer, Int. Chem. Eng. 23 (1983) 342–350.
[5] K. Sundmacher, L.K. Rihko, U. Hoffmann, Classification of reactive distillation processes by dimensionless numbers, Chem. Eng. Comm. 127 (1994) 151–167.
[6] J.S. Kirkaldy, Isothermal diffusion in multicomponent systems, Adv. Mater. Res. 4 (1970) 55–100.
[7] A. Rehfinger, U. Hoffmann, Kinetics of methyl tertiary butyl ether liquid phase synthesis catalyzed by ion exchange resin. I. Intrinsic rate expression in liquid phase activities, Chem. Eng. Sci. 45 (1990) 1605–1617.